The Universe at Infrared and Submillimeter Wavelengths

E. Dwek[1] , R. G. Arendt[2], D. J. Benford[1], J. C. Mather[1], S. H. Moseley[1], R. A. Shafer[1], & J. Staguhn[2]

ABSTRACT

Far infrared and submillimeter surveys offer unique information on the early stages of galaxy formation and evolution, and the cosmic history of star formation and metal enrichment. This paper presents various model results that can be used in the interpretation of far–IR and submm surveys with different diameter telescopes.

1. Introduction

Recent developments have shown that far–infrared (IR) and submillimeter (submm) observations can offer unique probes of the high– redshift universe. Detections and limits on the cosmic infrared background (CIB) (Hauser & Dwek 2001) show that a significant fraction of the energy generated in the universe is absorbed and reradiated by dust at far–IR and submm wavelengths. Deep surveys with the SCUBA instrument on the JCMT resolved most of the CIB at 850 μm, and revealed that most of the star formation at redshifts above ~ 2 takes place behind a veil of dust. The spectral energy distribution (SED) of galaxies peaks in the $\sim 60 - 140$ μm wavelength region. So even at large redshifts, submm observations sample the rising part of the galaxies' SED, and effect referred to as the negative K–correction. Thus, far–IR and submm surveys can be used to observe the early stages of galaxy formation and evolution, and provide the history of the star formation rate and metal enrichment in the universe.

2. The Construction of Galaxy Number Count Models

Here we will outline the ingredients for the construction of a simple galaxy number count model in the framework of a Backward Evolution (BE) model. BE models, as opposed to Forward Evolution, Semi–Analytical, or Cosmic Chemical Evolution models, extrapolate the spectral properties of galaxies in the local universe and their comoving number density to higher redshift, using some parametric form for their evolution (see Hauser & Dwek 2001 for a review of the various models). Within this framework, the model ingredients include: (1) a complete set of galactic

[1]Code 685, Laboratory for Astronomy & Solar Physics, NASA/Goddard Space Flight Center, Greenbelt, MD 20771

[1]SSAI, Code 685, NASA/Goddard Space Flight Center, Greenbelt, MD 20771

SED, representing galaxies of all morphological types and luminosities; (2) the galaxies' luminosity function (LF) in the local universe; (3) a prescription for the evolution of the galaxies SED and their LF with redshift; and (4) a cosmological model. The results presented here use the set of galaxies SEDs, their 15 μm LF, and the luminosity+density evolution model described by Chary & Elbaz (2001; CE01). The cosmology adopted here is that of a flat Λ dominated universe with $\Omega_m = 0.3$, $\Omega_\Lambda = 0.7$, and a Hubble constant of $H_0 = 75$ km s^{-1} Mpc^{-1}.

3. Model Results

Figure 1 shows the SED of select galaxies in the local universe, bracketing the luminosities assigned to the different type of galaxies: normal galaxies with $2.6 \times 10^8 < L_{IR}(L_\odot) < 1 \times 10^{11}$; luminous IR galaxies (LIRGs) with $1 \times 10^{11} < L_{IR}(L_\odot) < 1 \times 10^{12}$; and ultraluminous IR galaxies (ULIRGs) with $1 \times 10^{12} < L_{IR}(L_\odot) < 3.6 \times 10^{13}$. A noticeable trend in the figure is the diminishing strength of the broad unidetified IR bands (UIB), usually attributed to polycyclic aromatic hydrocarbon molecules or PAHs, as a function of the galaxies' IR luminosity.
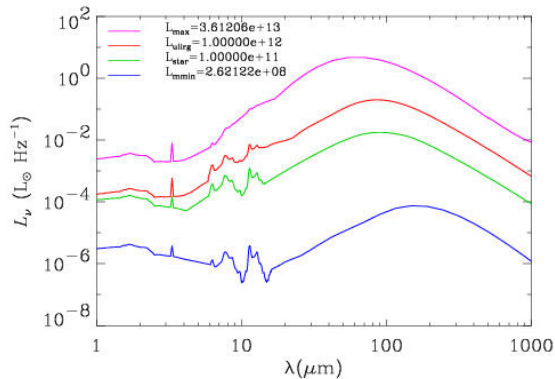

Fig. 1.— The SED of the galaxies bracketing normal galaxies, LIRGs, and ULIRGs in luminosity.

Figure 2 shows the observed flux of the galaxies depicted in the previous figure in the different IR passbands as a function of redshift. The behavior of the fluxes at redshifts above $z \approx 0.3$ is dominated by the movement of the UIB in and out of the band (at 15 μm only), and by the combined effects of the negative K-correction and luminosity evolution.

Figure 3 compares the calculated and observed differential galaxy number count, dN/dS, normalized to that expected in a Euclidean universe. The figure is essentially a reproduction of the results of the luminosity+density evolution model of Chary & Elbaz (2001). The model successfully reproduces the observed 15, 90, 170, and 850 μm galaxy number counts obtained with the *Infrared Space Observatory* (*ISO*) satellite (see Chary & Elbaz for a summary of the observations) and the SCUBA observations (Blaine et al. 1999). The figure also shows the contribution of the different

galaxy types to the number counts. The figure shows that ULIRG are the main contributors to the 850 μm number counts, whereas normal galaxies dominate the 15 and 90 μm bright galaxy counts, with LIRGs taking over the counts at lower fluxes.

Figure 4 depicts how the differential number count builds up with redshift. The vertical lines represent the 5σ confusion limts for (from right to left) 1, 2, 4, 8, and 16 m diameter telescopes. The cumulative flux from galaxies converges when the slope of $\mathrm{d}N\mathrm{d}S \times S^{5/2} \propto S^{1/2}$. Comparison of this figure with the data shown in the previous figure illustrates the redshift regions that contribute most to the observed number counts at each flux S_ν.

An important constraint on number count models is that the predicted cumulative flux from all sources be finite and converge to the cosmic IR background (CIB) at the different wavelengths. Figure 5 shows the cumulative contribution of all galaxy types to the CIB (left panel) and to the total number counts (right panel), as a function of wavelength. The shaded region in the left panel marks the limits and detections of the CIB summarized by Hauser & Dwek (2001).

In practice, the number of galaxies that can be resolved is limited by the confusion limit, defined as the flux below which an individual galaxy cannot be distinguished from fluctuations in the unresolved distribution of fainter galaxies. Figures 6 and 7 show, respectively, the contribution of resolved galaxies of different types to the CIB and the total number of galaxies using an 8 m diameter telescope (left panel), and a 16 m diameter telescope (right panel). Galaxy numbers and fluxes were integrated down to the 5σ confusion limit.

Figures 6 and 7 show that a 16 m diameter telescope will detect about 30% of the CIB at 500 μm, and about 3% of the total number of galaxies. The galaxies will comprise of about equal number of LIRGs and ULIRGs, at redshifts between ~ 1 and 4.

REFERENCES

Blain, A. W., Kneib, J. P., Ivison, R. J., & Smail I. 1999, ApJ, 512, L87

Chary, R., & Elbaz, D. 2001, ApJ, 556, 562
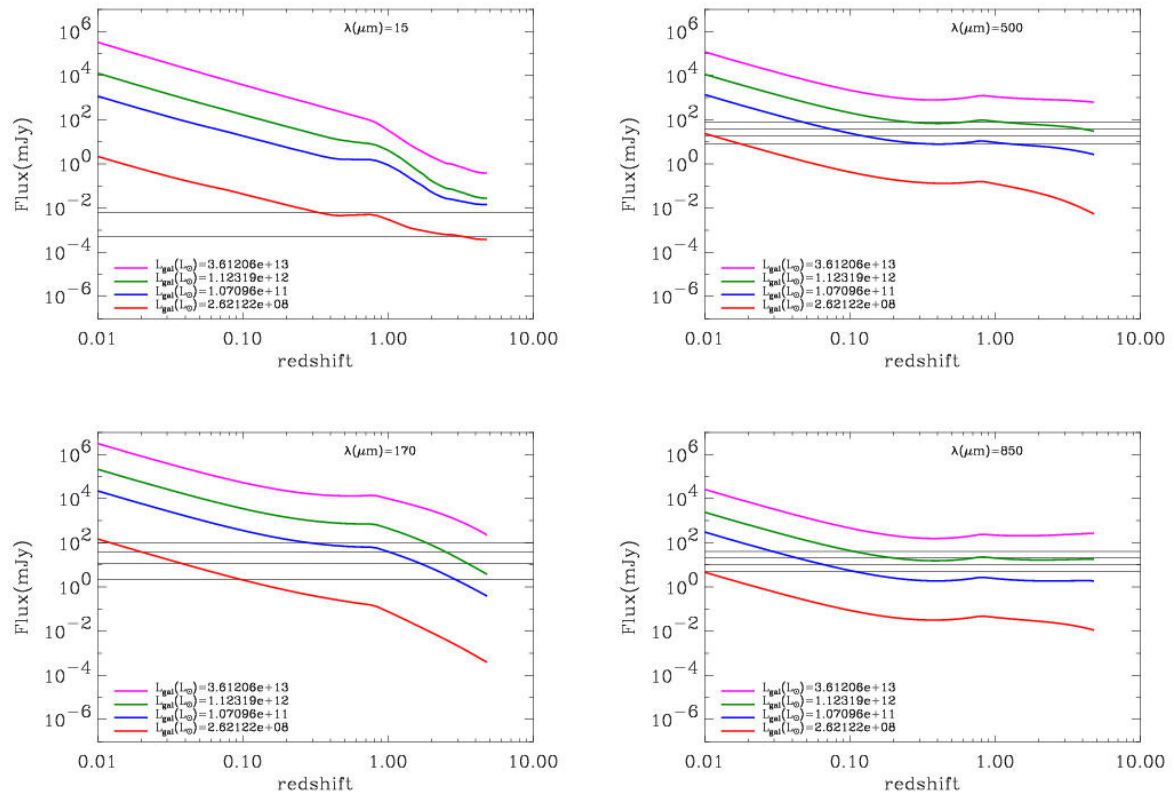
Hauser, M. G., & Dwek, E. 2001, ARA&A, 39, 249

Fig. 2.— The in–band flux of the select galaxies depicted in Figure 1 as a function of redshift. Note the effect of the UIB features at 15 μm, and the negative K–correction at 850 μm on the behavior of the flux with redshift.
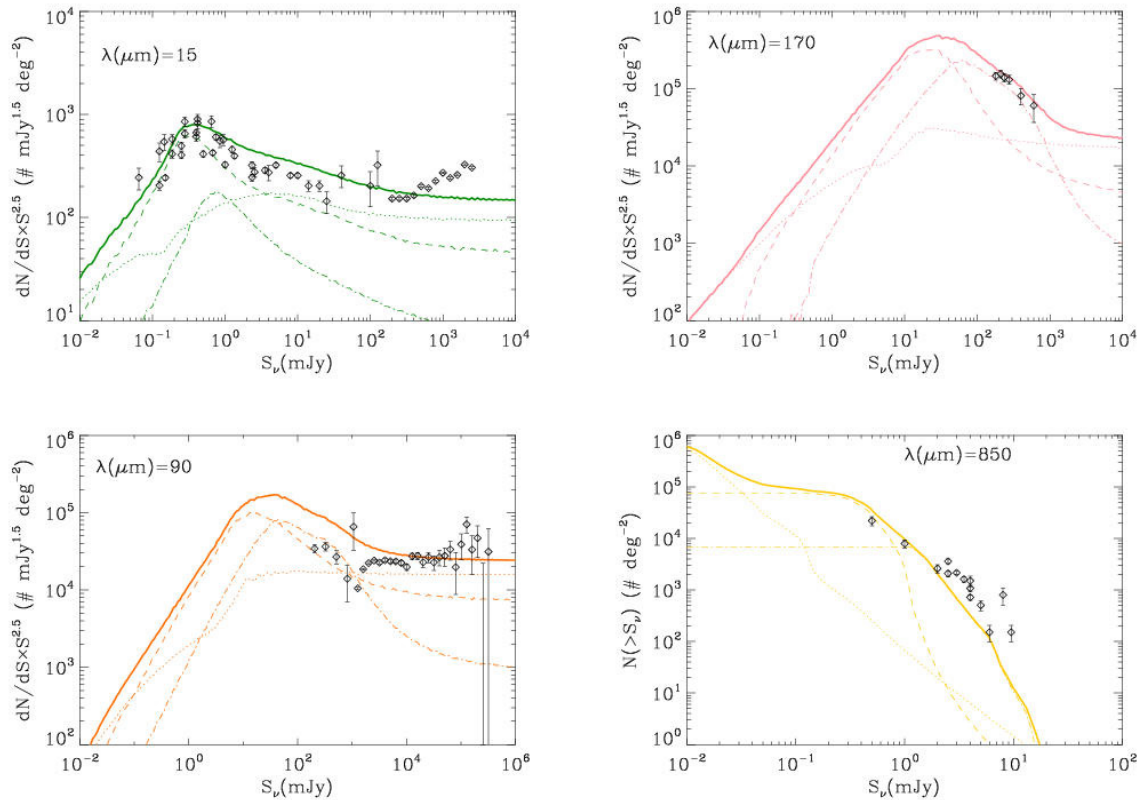
Fig. 3.— The differential number counts, calculated for the luminosity+density evolution model of Chary & Elbaz (2001), multiplied by $S^{5/2}$ is plotted as a function of galaxy flux density S_ν, and compared to observed counts. In a Euclidean universe with non–evolving galaxies, the plotted quantity should be a horizontal line. The figure also depicts the contribution of normal (......), LIRGs (——), and ULIRGs (-.-.-.-.) to the differential number counts.
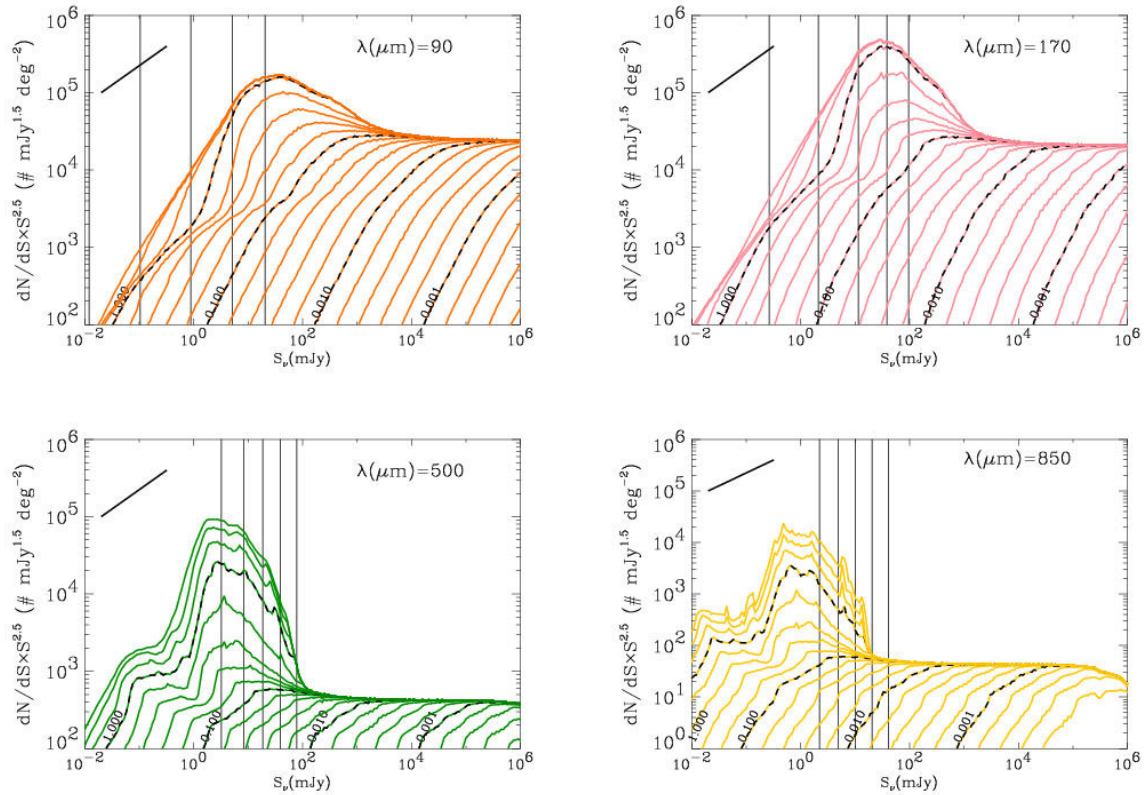
Fig. 4.— The buildup of the differential number counts with redshift. The dark contours represent redshifts of 0.001, 0.01, 0.1, and 1.0. The intervals between each pair of dark lines is divided into 5 equal logarithmic intervals. Vertical lines represent the confusion limits for various diameter telescopes. The dark line in the upper left corner has a slope of $S^{1/2}$, required for the cumuative light from the sources to converge. See text for more details.
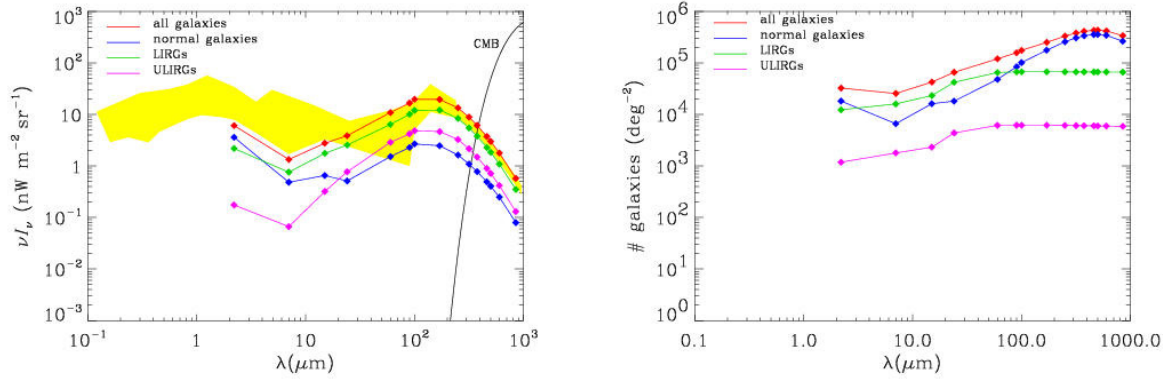
Fig. 5.— The contribution of the different type of galaxies to the CIB (left panel) and the total number of galaxies as a function of wavelength. The calculations assume that all galaxies in the universe are resolved, a zero–flux confusion limit.
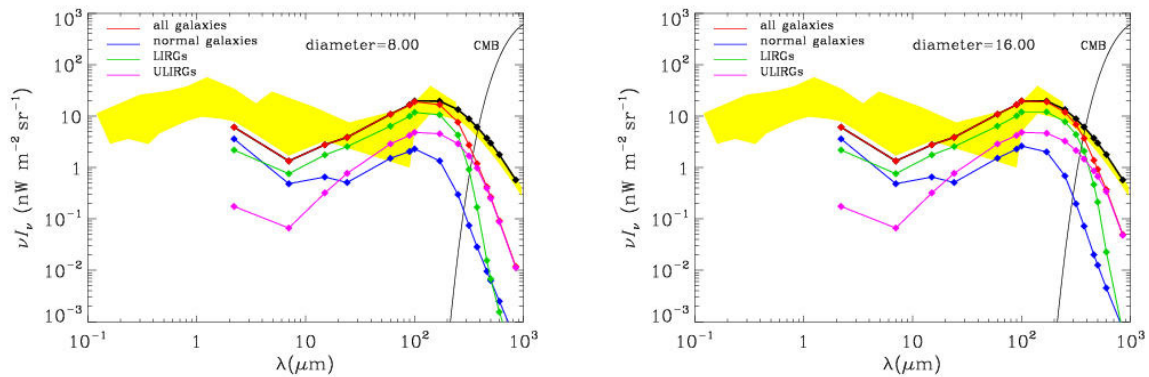

Fig. 6.— The contribution of resolved galaxies of different type to the CIB. Galaxy fluxes were integrated down to the 5σ confusion limit.
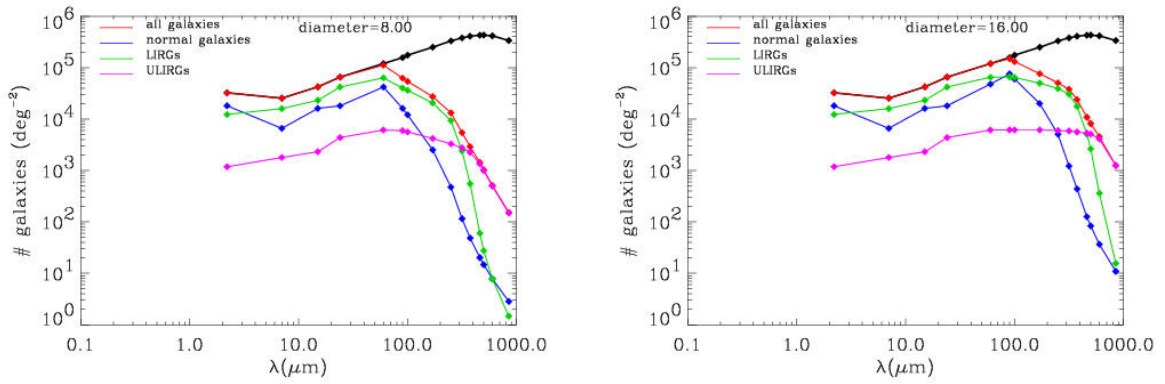
Fig. 7.— The contribution of resolved galaxies of different type to the total number of galaxies. Galaxies were counted down to the 5σ confusion limit.